materials

MDPI

Article

CoS_2/TiO_2 Nanocomposites for Hydrogen Production under UV Irradiation

Sivagowri Shanmugaratnam [1], Dhayalan Velauthapillai [1,*], Punniamoorthy Ravirajan [2], Alfred Antony Christy [3] and Yohi Shivatharsiny [4,*]

1 Faculty of Engineering and Science, Western Norway University of Applied Sciences, 5020 Bergen, Norway; sivagowrishanmugaratnam@gmail.com
2 Clean Energy Research Laboratory, Department of Physics, University of Jaffna, Jaffna 40000, Sri Lanka; pravirajan@gmail.com
3 Department of Natural Science, University of Agder, 4630 Kristiansand, Norway; alfred.christy@uia.no
4 Department of Chemistry, University of Jaffna, Jaffna 40000, Sri Lanka
* Correspondence: Dhayalan.Velauthapillai@hvl.no (D.V.); srtharsha12@gmail.com (Y.S.)

Received: 22 October 2019; Accepted: 22 November 2019; Published: 24 November 2019

Abstract: Transition metal chalcogenides have intensively focused on photocatalytic hydrogen production for a decade due to their stronger edge and the quantum confinement effect. This work mainly focuses on synthesis and hydrogen production efficiencies of cobalt disulfide (CoS_2)-embedded TiO_2 nanocomposites. Materials are synthesized by using a hydrothermal approach and the hydrogen production efficiencies of pristine CoS_2, TiO_2 nanoparticles and CoS_2/TiO_2 nanocomposites are compared under UV irradiation. A higher amount of hydrogen production (2.55 mmol g^{-1}) is obtained with 10 wt.% CoS_2/TiO_2 nanocomposite than pristineTiO_2 nanoparticles, whereas no hydrogen production was observed with pristine CoS_2 nanoparticles. This result unveils that the metal dichalcogenide–CoS_2 acts as an effective co-catalyst and nanocrystalline TiO_2 serves as an active site by effectively separating the photogenerated electron–hole pair. This study lays down a new approach for developing transition metal dichalcogenide materials with significant bandgaps that can effectively harness solar energy for hydrogen production.

Keywords: transition metal chalcogenides; titania; hydrothermal; hydrogen; water splitting

1. Introduction

Depletion of fossil fuel deserves utilization of hydrogen as a renewable energy source. It could be one of the promising energy sources alternative to fossil fuels in meeting the energy demand of the current world population. Currently, the major hydrogen production is from steam-methane reforming and thermal cracking of natural gas, and coal gasification, which cannot alleviate the emission of greenhouse gases [1]. Electrolysis is another method, which is being used to produce hydrogen. Electrochemical reduction of water [2–4] is an ecofriendly method and exhibits high-purity (99.999%) of hydrogen [5]; in addition, this is a key to many clean energy technologies. Although there have been several methods used to produce hydrogen, photocatalytic hydrogen generation have gained much attention these days. This technique integrates solar energy collection together with water splitting, therefore, it is a more cost-effective method compared with the water electrolysis process. Unfortunately, only a small percentage of hydrogen is produced from the photocatalytic method under solar extended irradiation. Therefore, the development of new materials for sustainable hydrogen production is necessary to overcome the detrimental environmental impacts. In the past decade, different photocatalyst materials, such as TiO_2 [6–8], ZnO [9], CdS [10,11], WS_2 [12,13], mixed oxides [14,15], perovskites [16,17], dye and metal doped oxide materials [18,19] have been used

as phototcatalysts for environmental remediation and energy production, such as water splitting applications. In particular, catalysts contain noble metals, such as Pt have also been utilized in the state-of-the-art hydrogen evolution reaction. However, large scale hydrogen production is limited with these catalysts [20–22]. Among the materials studied, TiO_2 has been considered as the golden standard due to its significant characteristics that include photochemical stability, low toxicity, relative affordability, and ease of preparation [23]. Although the bandgap energy of TiO_2 necessitates the use of UV irradiation, composites of TiO_2 with co-catalysts, such as transition metal chalcogenides (TMCs), enable the catalysts to absorb visible light abundant in solar irradiation [24]. In this regard, TMCs have gained much attention among the research community in the field of lithium ion batteries, solar cells and hydrogen evolution, due to their significant characteristic features that include indirect bandgaps, optoelectronic properties and stability [24]. In addition, nanodots (quantum dots)/nano structures of these metal chalcogenides show stronger edge effects, and the quantum confinement effect make them suitable to be utilized under solar simulated irradiation [24,25]. The transition metal chalcogenides can be synthesized by employing different techniques, such as one-pot wet chemical method [10], impregnation–sulfidation [11], simple microwave-assisted solvothermal process [26], ion exchange and precipitation methods [27], and hydrothermal method [28]. Several studies on bare transition metal chalcogenides (MoS_2, NiS_2, WS_2, CdS and CoS) for the hydrogen evolution reaction (HER) and oxygen reduction reactions (ORR) are reported [29–32], however, most of these studies mainly focused on electrochemical water splitting. Co-catalysts, such as, reduced graphene oxides [33], metal oxides [34], dyes, for example, Porphyrin (Zn(II)-5,10,15,20-tetrakis(4-carboxyphenyl)-porphyrin (ZnTCPP)) [19], graphene [35], metals [36], and $CdLa_2S_4$ nanocrystals [37] were used to enhance the rate of HER. Inorganic crystals with desired properties can be used as excellent candidates for HER. It was reported that the first-row transition metal chalcogenides (MS_2; where M = Fe, Co, Ni) exhibit excellent catalytic properties for HER due to their pyrite or marcasite structure, in which the metal atoms are octahedrally bonded to adjacent S atoms. Stability is an important criterion in the development of catalysts [30,38–45]. In this regard, computational modelling was also employed on these metal chalcogenide materials to evaluate their structural properties for photocatalytic water splitting and hydrogen production [46]. In particular, MoS_2 has been utilized with other elements via adsorption or intercalation of a cation, such as Li for electrochemical water splitting [46]. In another modelling work, a comparative study was done between WS_2 and MoS_2 in electrocatalytic water splitting [12]; In an experimental study, Yuexiang Li et al. reported hydrogen production of 99 μmol h^{-1} with MoS_2 loaded on the composites of reduced graphene oxide and CdS, and this was found to be over 20 times higher than the bare CdS. CoS_2 doped with Mn [47] and Al [48] used for electrocatalytic HER [49].

Although all the reported work on TMC-embedded TiO_2 mainly focused on the electrochemical water splitting and computer modelling, to the best of our knowledge, no experimental study on TMC-embedded TiO_2 for heterogeneous hydrogen production over extended solar irradiation has been reported yet. This study focuses on the synthesis of CoS_2 (metal chalcogenide)-embedded TiO_2 nanocomposite, and the impact of doping CoS_2 with TiO_2 in hydrogen evolution under UV irradiation.

2. Materials and Methods

2.1. Materials

Without further purification, titanium isopropoxide, 98+% (Sigma-Aldrich Norway AS, Oslo, Norway) was employed as the precursor for TiO_2 preparation, Cobalt (II) nitrate hexahydrate, 99% pure (Sigma-Aldrich Norway AS) was utilized as the cobalt precursor, and $Na_2S_2O_3$ (Sigma-Aldrich Norway AS) as sulfur source. PHARMCO-AAPER Ethyl alcohol (200 Proof; Absolute, anhydrous, Sigma-Aldrich Norway AS) was used as solvent and deionized water (resistivity >18 Ω·cm, Velp/AREC, VELP Scientifica Srl, Usmate (MB), Italy) was used to prepare the solution mixtures.

2.2. Methods

2.2.1. Synthesis

(1) Titanium dioxide

Nanocrystalline titanium dioxide material was prepared under hydrothermal condition using sol-gel technique. In a typical synthesis, 32.5 mL of ethanol was acidified with 0.3 mL concentrated HNO_3 (Sigma-Aldrich, Oslo, Norway) in a Teflon liner and stirred at a constant speed (300 rpm, Velp/AREC, VELP Scientifica Srl,). 6.60 mL of titanium (iv) isopropoxide was added drop wise into it with continuous stirring, Finally, 3.0 mL of water was added to the above solution. Then, it was transferred into an autoclave (AUTOCLAVE-PTFE-0100, TECINSTRO, Maharashtra, India) and kept at 180 °C for 9 hours. The final material was heated at 500 °C for 3 h.

(2) CoS_2 embedded TiO_2 nanocomposite

118.24 mg of $Co(NO_3)_2$ and 192.72 mg of $Na_2S_2O_3$ were added in to a 100 mL aqueous solution containing deionized water and ethanol in 2:1 ratio under constant stirring (300 rpm) for 30 min. Finally, required amount of TiO_2 was dispersed into above solution and the resulting mixture was hydrothermally treated at 180 °C to prepare 10 wt.% of CoS_2 embedded TiO_2 material. Similar conditions were followed in the preparation of pristine CoS_2 nanoparticles without adding titanium dioxide.

2.2.2. Characterization

Synthesized materials were subjected to different characterization techniques, such as Powder X-ray Diffraction (P-XRD, Ultima IV Rigaku, USA) Method, Diffuse Reflectance Spectra (DRS Cary 100 Bio UV–Visible spectrophotometer, Santa Clara, CA, USA) and Scanning Electron Microscopy (SEM, Oxford instrument, NanoAnalysis, Concord, MA, USA). P-XRD patterns were recorded on a Rigaku Ultima IV instrument (Scottsdale, AZ, USA) with Cu Kα radiation (λ = 1.5408 Å) at ambient temperature, under the following operating conditions; accelerating voltage of 40 kV; emission current of 44 mA; scanned range (2θ) between 20° and 80° with a step size of 0.02°, and a scan speed of 1°/min. DRS were acquired using a Cary 100 Bio UV–Visible spectrophotometer, and the SEM images were captured on an Oxford instrument.

2.2.3. Photocatalytic Hydrogen Evolution

The photocatalytic experiments were carried out for pristine TiO_2, CoS_2 and CoS_2/TiO_2. Catalysts were suspended in a solution containing 1.5 mL of H_2O and 0.5 mL of methanol as a scavenging agent. The suspension was degassed for 30 minutes with high-purity argon prior to irradiation. The suspensions were continuously stirred throughout the course of the experiment. A 300 W Xenon lamp (Oriel light source, Xenon arc lamp, Newport 1000W, CA, USA) with an appropriate filter was used as the source of UV radiation. The amount of H_2 produced was measured by gas chromatography (SRI 8610 C, SRI instruments, Torrance, CA, USA) equipped with a molecular sieve column and a TCD (Thermal Conductivity detector), and the amount of hydrogen produced was quantified by using a calibration curve prepared previously.

3. Results and Discussion

3.1. Characterization of Materials

The powder XRD patterns of the pristine CoS_2, TiO_2, and 10 wt.% CoS_2/TiO_2 nanocomposites are shown in Figure 1. The peaks observed at the 2 theta values of 26.04°, 31.58°, 37.08°, 40.34°, 45.34° and 55.1° are due to (111), (200), (210), (211), (220) and (311) diffraction planes of CoS_2 (PDF Card No.: 9007682). The peaks at 2θ of 25.50°, 37.76°, 48.10°, 53.88°, 55.84° and 62.90° due to the (101), (004), (200), (105), (211) and (204) diffraction planes confirm the formation of TiO_2 anatase phase

(JCPDS 21-1272) [50]. Combination of CoS_2 and TiO_2 peaks observed with the 10 wt.% CoS_2/TiO_2 nanocomposite confirms good impregnation of CoS_2 on TiO_2.

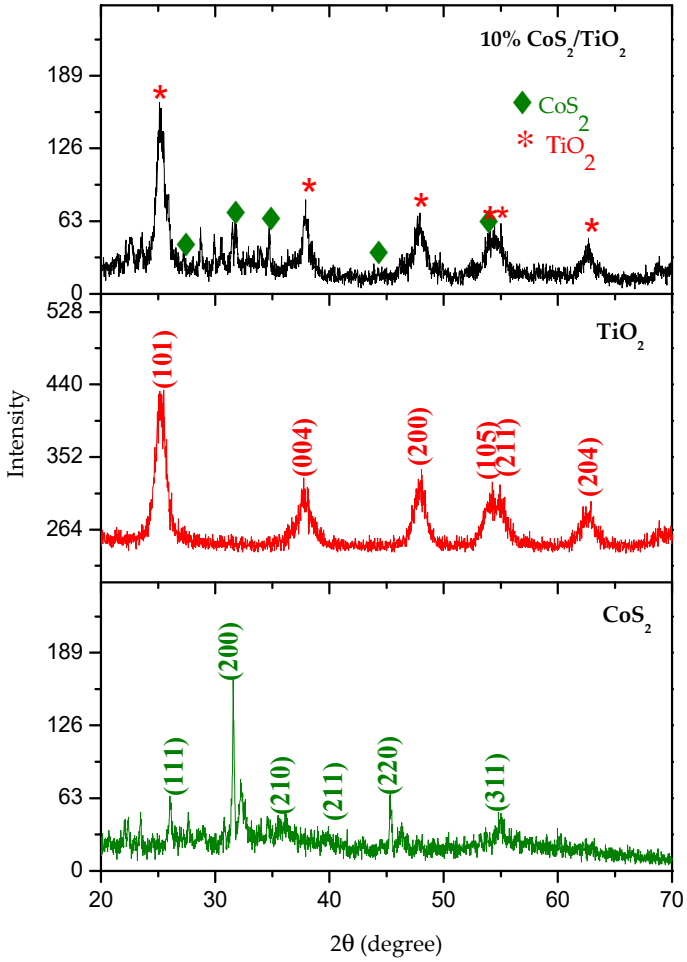

Figure 1. XRD patterns of the pristine CoS_2, TiO_2, and 10 wt.% CoS_2/TiO_2 nanocomposite.

Scanning electron microscopic images of blank CoS_2 (a,b), TiO_2 (c,d) and 10 wt.% CoS_2/TiO_2 (e,f) are illustrated in Figure 2. It can clearly be seen from Figure 2a,b that the bare CoS_2 shows an aggregation, which is surrounded by flake like structures. An irregular 3D block-like structure covered with spongy like particles was attained for TiO_2 nanocomposite and is shown in Figure 2c, and the zoom in image (Figure 2d) clearly illustrates the aggregated particles which have spongy-like structures. The mixed composite, CoS_2/TiO_2 also exhibits the aggregation, in which the zoom in image (Figure 2f) shows the hexagonal rod like structure decorated with spongy like materials [51].

The bandgap energies for the pristine CoS_2, TiO_2 and 10 wt.% CoS_2/TiO_2 nanocomposite materials corresponding to the absorbance spectra of powder samples (Figure 3a), were estimated by using the Tauc plot (Figure 3b), which was transformed via the Kubelka–Munk function [52], $[F(R_\infty)E]^n$ vs. E, when n = 0.5, for a direct allowed transition $(K = F(R_\infty))$. Estimates derived from the Tauc plots by extrapolating the steep portion of the plot in Figure 3b to the x-axis suggest that the bandgaps of the pristine CoS_2 (2.5 eV), TiO_2 (3.2 eV) and CoS_2 embedded TiO_2 nanocomposite (3.4 eV) materials lie in the range between 2.4 and 3.4 eV.

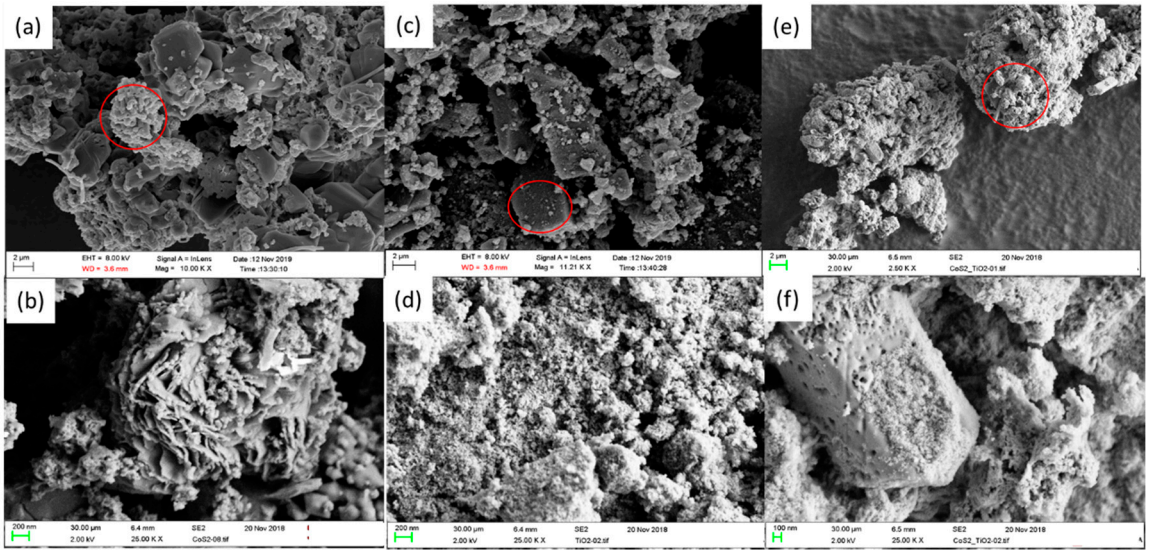

Figure 2. SEM images of the CoS_2 (**a**,**b**), TiO_2 (**c**,**d**), and 10 wt.% CoS_2/TiO_2 (**e**,**f**) nanocomposite.

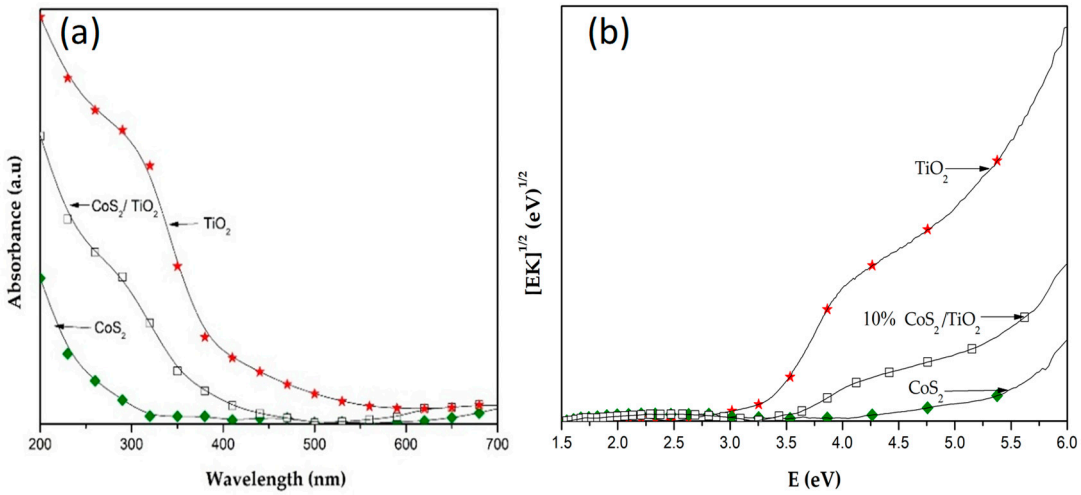

Figure 3. (**a**) Absorbance from diffuse reflectance spectra and (**b**) Tauc plots of pristine CoS_2, TiO_2 and 10 wt.% CoS_2/TiO_2 nanocomposite.

3.2. Hydrogen Evolution

The amount of hydrogen evolved in the presence of UV irradiation is tabulated and compared with what is reported in the literature in Table 1. Transition metal chalcogenides, including MoS_2, NiS, SnS_2, WS_2, and CdS, have been extensively explored for photocatalytic water splitting [11,24,36,49], since they are usually inexpensive, stable, and easily prepared on a large scale for practical applications. To improve the efficiency of TMCs on hydrogen evolution elemental doping, heterojunctions, and nano structuring have been explored. In this regard, metal chalcogenides have been doped with other components, such as reduced graphene oxide, graphene, dyes, and TiO_2 using different experimental conditions.

Table 1. Amount of hydrogen evolved with different transition metal Chalcogenides: A comparison.

Material	Synthesis Method	Rate of Hydrogen Evolution	Sacrificial Agent	Reference	
2D SnS_2/g-C_3N_4 (5 wt.% SnS_2/g-C_3N_4)	Hydrothermal method	0.97 mmol h^{-1} g^{-1}	10 vol% TEOA and 3 wt.% $H_2Pt_2Cl_6{\cdot}6H_2O$	Enzhou Liu et al., 2018	[53]
Te/SnS_2/Ag	Hydrothermal method	0.33 mmol h^{-1}	-	Changzeng Yan et al., 2017	[36]
SnS_2 Nanosheets	Solvothermal	1.06 mmol h^{-1} g^{-1}	0.1 M Na_2S 0.1M $Na_2S_2O_3$	Jing yu et al., 2014	[54]
CdS/ WS_2	Impregnation-sulfidation	0.42 mmol h^{-1}	Latic acid solution	Zong et al., 2011	[11]
Dye-Sensitized NiS_x/ graphene (in EY/G)	Insitu chemical deposition method	0.04 mmol h^{-1}	-	Chao Kong et al., 2014	[55]
Dye-Sensitized NiS_x/ graphene (in EY/NiS_x/G)	Insitu chemical deposition method	0.34 mmol h^{-1}	-	Chao Kong et al., 2014	[55]
MoS_2/ RGO and CdS (pH11-MoS_2/rGO 1.5/CdS)	Photoreduction method	0.10 mmol h^{-1}	10 vol.% Latic acid solution	Yuexiang Li et al., 2014	[49]
MoS_2/Graphene	Hydrothermal	1.80 mmol h^{-1}	Na_2S-$Na_2S_2O_3$ solution	Chang et al., 2014	[35]
MoS_2 quantum dots/TiO_2 nanotube arrays	Electrodeposition	0.07 mmol cm^{-2} h^{-1} 0.05 mmol cm^{-2} h^{-1} 0.02 mmoL cm^{-2} h^{-1}	-	Qun Wang et al., 2018	[24]
ZnTCPP-MoS_2 /TiO_2 (1.00 wt.% MoS_2 on TiO_2)	Hydrothermal	0.10 mmol h^{-1}	0.2 M triethanolamine (TEOA) aqueous	Youngjun Yuan et al., 2015	[19]
10 wt.% CoS_2/TiO_2	Hydrothermal	2.55 mmol g^{-1}	Methanol	This work	

For example, Qun Wang et al. worked on MoS_2 quantum dots-doped TiO_2 for hydrogen evolution reaction in under different experimental condition, and the rate of hydrogen evolution was found to be 0.05 mmol cm^{-2} h^{-1} [24]. In another study, Youngjun Yuan et al. used ZnTCPP-MoS_2 /TiO_2 material for HER (Hydrogen Evolution Reaction), where 0.10 mmol h^{-1} of hydrogen evolved with 1.00 wt.% of MoS_2 on TiO_2 material [19]. In line with these studies, the results from our study on metal chalcogenide-TiO_2 nanocomposites showed that 10 wt.% CoS_2 embedded on TiO_2 nanocomposites synthesized by hydrothermal method was the excellent candidate for the photocatalytic HER with better hydrogen evolution rate of 2.55 mmol g^{-1}. Pristine CoS_2 alone showed no activity towards hydrogen production even after 4 hours of irradiation, whereas the TiO_2 materials exhibited 1.88 $mmolg^{-1}$ of hydrogen under the same experimental conditions. The reason for this observation can be correlated with the bandgap energies of the materials. The CoS_2/TiO_2 materials with highest activity exhibit bandgap of 3.4 eV, whereas the pristine TiO_2 exhibits bandgap of 3.2 eV. Under UV irradiation, the electron-hole pair formed on the nanocomposites was effectively separated due to the bandgap >3 eV. However, in the case of pristine CoS_2 (Bandgap of 2.5 eV), it can be concluded that the faster recombination rate of photogenerated electrons and holes hinder the formation of hydrogen effectively, and, thus, there is no activity observed with this catalyst, but CoS_2 nanoparticles act as a co-catalyst in the nanocomposite of CoS_2/TiO_2 materials to enhance the hydrogen production by exciting more electrons to the surface of titanium dioxide.

4. Conclusions

Pristine CoS_2 and TiO_2, and CoS_2/TiO_2 nanocomposites were successfully synthesized via a hydrothermal method using titanium(iv)isopropoxide, $Co(NO_3)_2$ and $Na_2S_2O_3$ as precursors. The mixed COS_2/TiO_2 nanocomposite exhibits a high hydrogen production value of 2.55 mmol g^{-1}, whereas the pristine CoS_2 material was found to be inactive due to its very low bandgap energy. The TiO_2 material shows an intermediate hydrogen production of 1.88 mmol g^{-1}. In summary, the hydrogen production seems to depend on the band gap energy of the catalysts, and the CoS_2 may assist to effectively separate the electron-hole pair forms in the mixed nanocomposite, and thus, results in a higher value of hydrogen production.

Author Contributions: Conceptualization, Y.S, and S.S.; methodology, S.S. and Y.S.; software, S.S., and Y.S.; validation, S.S., A.A.C., D.V., P.R. and Y.S.; formal analysis, S.S. and Y.S.; investigation, S.S. and S.R.; resources, Y.S., P.R., and D.V.; data curation, S.S. and Y.S.; writing—original draft preparation, S.S.; writing—review and editing, Y.S., D.V., P.R., and A.A.C.; visualization, S.S.; supervision, A.A.C., D.V., P.R., and Y.S.; project administration, P.R. and D.V.; funding acquisition, P.R. and D.V.

Funding: This research was funded by Capacity Building and Establishment of a Research Consortium (CBERC) project, grant number LKA-3182-HRNCET and Higher Education and Research collaboration on Nanomaterials for Clean Energy Technologies (HRNCET) project, and grant number NORPART/2016/10237.

Acknowledgments: Authors would like to acknowledge Aravind Baride (University of South Dakota), who assisted with the SEM analysis. Y.S would like to thank Ranjit Koodali (University of South Dakota) for allowing her to utilize his lab to do the hydrogen evolution measurements.

Conflicts of Interest: The authors declare no conflict of interest.

References

1. Kudo, A.; Miseki, Y. Heterogeneous photocatalyst materials for water splitting. *Chem. Soc. Rev.* **2009**, *38*, 253–278. [CrossRef] [PubMed]
2. Cook, T.R.; Dogutan, D.K.; Reece, S.Y.; Surendranath, Y.; Teets, T.S.; Nocera, D.G. Solar Energy Supply and Storage for the Legacy and Nonlegacy Worlds. *Chem. Rev.* **2010**, *110*, 6474–6502. [CrossRef] [PubMed]
3. Walter, M.G.; Warren, E.L.; Mckone, J.R.; Boettcher, S.W.; Mi, Q.; Santori, E.A.; Lewis, N.S. Solar Water Splitting Cells. *Chem. Rev.* **2010**, *110*, 6446–6473. [CrossRef] [PubMed]
4. Lewis, N.S.; Nocera, D.G. Powering the planet: Chemical challenges in solar energy utilization. *Proc. Natl. Acad. Sci. USA* **2006**, *103*, 15729–15735. [CrossRef] [PubMed]
5. Shiva Kumar, S.; Himabindu, V. Hydrogen production by PEM water electrolysis—A review. *Mater. Sci. Energy Technol.* **2019**, *2*, 442–454. [CrossRef]
6. Yin, Y.; Jin, Z.; Hou, F. Enhanced solar water-splitting efficiency using core/sheath heterostructure CdS/TiO2 nanotube arrays. *Nanotechnology* **2007**, *18*, 495608. [CrossRef]
7. Kim, S.B.; Hong, S.C. Kinetic study for photocatalytic degradation of volatile organic compounds in air using thin film TiO_2 photocatalyst. *Appl. Catal. B Environ.* **2002**, *35*, 305–315. [CrossRef]
8. Matthews, R.W. Photooxidative degradation of coloured organics in water using supported catalysts. TiO_2 on sand. *Water Res.* **1991**, *25*, 1169–1176. [CrossRef]
9. Chakrabarti, S.; Dutta, B.K. Photocatalytic degradation of model textile dyes in wastewater using ZnO as semiconductor catalyst. *J. Hazard. Mater.* **2004**, *112*, 269–278. [CrossRef]
10. Chen, J.; Wu, X.J.; Yin, L.; Li, B.; Hong, X.; Fan, Z.; Chen, B.; Xue, C.; Zhang, H. One-pot synthesis of CdS nanocrystals hybridized with single-layer transition-metal dichalcogenide nanosheets for efficient photocatalytic hydrogen evolution. *Angew. Chem. Int. Ed.* **2015**, *54*, 1210–1214. [CrossRef] [PubMed]
11. Zong, X.; Han, J.; Ma, G.; Yan, H.; Wu, G.; Li, C. Photocatalytic H_2 evolution on CdS loaded with WS_2 as cocatalyst under visible light irradiation. *J. Phys. Chem. C* **2011**, *115*, 12202–12208. [CrossRef]
12. Chen, T.Y.; Chang, Y.H.; Hsu, C.L.; Wei, K.H.; Chiang, C.Y.; Li, L.J. Comparative study on MoS_2 and WS_2 for electrocatalytic water splitting. *Int. J. Hydrog. Energy* **2013**, *38*, 12302–12309. [CrossRef]
13. Feng, C.; Huang, L.; Guo, Z.; Liu, H. Synthesis of tungsten disulfide (WS_2) nanoflakes for lithium ion battery application. *Electrochem. Commun.* **2007**, *9*, 119–122. [CrossRef]

14. Pirashanthan, A.; Murugathas, T.; Robertson, N.; Ravirajan, P.; Velauthapillai, D. A Quarterthiophene-Based Dye as an Efficient. *Polymers* **2019**, *11*, 1752. [CrossRef] [PubMed]
15. Mugunthan, E.; Saidutta, M.B.; Jagadeeshbabu, P.E. Photocatalytic degradation of diclofenac using TiO_2–SnO_2 mixed oxide catalysts. *Environ. Technol. (UK)* **2019**, *40*, 929–941. [CrossRef]
16. Kim, H.G.; Hwang, D.W.; Kim, J.; Kim, Y.G.; Lee, J.S. Highly donor-doped (110) layered perovskite materials as novel photocatalysts for overall water splitting. *Chem. Commun.* **1999**, *2*, 1077–1078. [CrossRef]
17. Kanazawa, T.; Nozawa, S.; Lu, D.; Maeda, K. Structure and Photocatalytic Activity of $PdCrO_x$ Cocatalyst on $SrTiO_3$ for Overall Water Splitting. *Catalysts* **2019**, *9*, 59. [CrossRef]
18. Jafari, T.; Moharreri, E.; Amin, A.S.; Miao, R.; Song, W.; Suib, S.L. Photocatalytic water splitting—The untamed dream: A review of recent advances. *Molecules* **2016**, *21*, 900. [CrossRef]
19. Yuan, Y.; Lu, H.; Ji, Z.; Zhong, J.; Ding, M.; Chen, D.; Li, Y.; Tu, W.; Cao, D.; Yu, Z.; et al. Enhanced visible-light-induced hydrogen evolution from water in a noble-metal-free system catalyzed by ZnTCPP-$MoSTiO_2$ assembly. *Chem. Eng. J.* **2015**, *275*, 8–16. [CrossRef]
20. Gasteiger, H.A.; Shao-horn, Y.; Sheng, W.; Gasteiger, H.A.; Shao-horn, Y. Hydrogen Oxidation and Evolution Reaction Hydrogen Oxidation and Evolution Reaction Kinetics on Platinum: Acid vs Alkaline Electrolytes. *J. Electrochem. Soc.* **2010**, *157*, B1529–B1536.
21. Greeley, J.; Nørskov, J.K.; Kibler, L.A.; El-aziz, A.M.; Kolb, D.M. Hydrogen Evolution Over Bimetallic Systems: Understanding the Trends. *Chem. Phys. Chem.* **2006**, *7*, 1032–1035. [CrossRef] [PubMed]
22. Schuldiner, S. Hydrogen Overvoltage on Bright Platinum. *J. Electrochem. Soc.* **1952**, *99*, 488–494. [CrossRef]
23. Hamidi, F. TiO_2 -based Photocatalytic Cementitious Composites: Materials, Properties, Influential Parameters, and Assessment Techniques. *Nanomaterials* **2019**, *9*, 1444. [CrossRef] [PubMed]
24. Wang, Q.; Huang, J.; Sun, H.; Ng, Y.H.; Zhang, K.Q.; Lai, Y. MoS_2 Quantum Dots@TiO_2 Nanotube Arrays: An Extended-Spectrum-Driven Photocatalyst for Solar Hydrogen Evolution. *Chem. Sus. Chem.* **2018**, *11*, 1708–1721. [CrossRef]
25. Zheng, L.; Zhang, W.; Xiao, X. Preparation of titanium dioxide/tungsten disulfide composite photocatalysts with enhanced photocatalytic activity under visible light. *Korean J. Chem. Eng.* **2016**, *33*, 107–113. [CrossRef]
26. Liu, H.; Su, Y.; Chen, P.; Wang, Y. Microwave-assisted solvothermal synthesis of 3D carnation-like SnS 2 nanostructures with high visible light photocatalytic activity. *J. Mol. Catal. A Chem.* **2013**, *378*, 285–292. [CrossRef]
27. Nezamzadeh-Ejhieh, A.; Moeinirad, S. Heterogeneous photocatalytic degradation of furfural using NiS-clinoptilolite zeolite. *Desalination* **2011**, *273*, 248–257. [CrossRef]
28. Huerta-Flores, A.M.; Torres-Martínez, L.M.; Moctezuma, E.; Singh, A.P.; Wickman, B. Green synthesis of earth-abundant metal sulfides (FeS_2, CuS, and NiS_2) and their use as visible-light active photocatalysts for H_2 generation and dye removal. *J. Mater. Sci. Mater. Electron.* **2018**, *29*, 11613–11626. [CrossRef]
29. Fang, W.; Liu, D.; Lu, Q.; Sun, X.; Asiri, A.M. Nickel promoted cobalt disulfide nanowire array supported on carbon cloth: An efficient and stable bifunctional electrocatalyst for full water splitting. *Electrochem. Commun.* **2016**, *63*, 60–64. [CrossRef]
30. Desheng, K.; Cha, J.J.; Wang, H.-T.; Hye, R.L.; Yi, C. First-row transition metal dichalcogenide catalysts for hydrogen evolution reaction. *Energy Environ. Sci.* **2013**, *6*, 3553–3558.
31. Susac, D.; Zhu, L.; Teo, M.; Sode, A.; Wong, K.C.; Wong, P.C.; Parsons, R.R.; Bizzotto, D.; Mitchell, K.A.R.; Campbell, S.A. Characterization of FeS_2 -Based Thin Films as Model Catalysts for the Oxygen Reduction Reaction. *J. Phys. Chem. C* **2007**, *111*, 18715–18723. [CrossRef]
32. Feng, Y.; He, T.; Alonso-vante, N. Electrochimica Acta Oxygen reduction reaction on carbon-supported $CoSe_2$ nanoparticles in an acidic medium. *Electrochim. Acta* **2009**, *54*, 5252–5256. [CrossRef]
33. Li, Y.; Wang, H.; Xie, L.; Liang, Y.; Hong, G.; Dai, H. MoS_2 nanoparticles grown on graphene: An advanced catalyst for the hydrogen evolution reaction. *J. Am. Chem. Soc.* **2011**, *133*, 7296–7299. [CrossRef]
34. Khan, Z.; Chetia, T.R.; Vardhaman, A.K.; Barpuzary, D.; Sastri, C.V.; Qureshi, M. Visible light assisted photocatalytic hydrogen generation and organic dye degradation by CdS-metal oxide hybrids in presence of graphene oxide. *RSC Adv.* **2012**, *2*, 12122–12128. [CrossRef]
35. Chang, K.; Mei, Z.; Wang, T.; Kang, Q.; Ouyang, S.; Ye, J. MoS_2/graphene cocatalyst for efficient photocatalytic H_2 evolution under visible light irradiation. *ACS Nano* **2014**, *8*, 7078–7087. [CrossRef]

36. Yan, C.; Xue, X.; Zhang, W.; Li, X.; Liu, J.; Yang, S.; Hu, Y.; Chen, R.; Yan, Y.; Zhu, G.; et al. Well-designed Te/SnS_2/Ag artificial nanoleaves for enabling and enhancing visible-light driven overall splitting of pure water. *Nano Energy* **2017**, *39*, 539–545. [CrossRef]
37. Yuan, Y.P.; Cao, S.W.; Yin, L.S.; Xu, L.; Xue, C. NiS_2 Co-catalyst decoration on $CdLa_2S_4$ nanocrystals for efficient photocatalytic hydrogen generation under visible light irradiation. *Int. J. Hydrog. Energy* **2013**, *38*, 7218–7223. [CrossRef]
38. Chen, W.; Sasaki, K.; Ma, C.; Frenkel, A.I.; Marinkovic, N.; Muckerman, J.T.; Zhu, Y.; Adzic, R.R. Hydrogen-Evolution Catalysts Based on Non-Nobel Metal Nickel–Molybdenum Nitride Nanosheets. *Angew. Chem. Int. Ed.* **2012**, *51*, 6131–6135. [CrossRef]
39. Chen, W.-F.; Wang, C.-H.; Sasaki, K.; Marinkovic, N.; Xu, W.-Q.; Muckerman, J.; Zhu, Y.-M.; Adzic, R.R. Nanostructured Molybdenum Carbide as Pt-free Catalysts for Hydrogen Evolution. *Electrochem. Soc.* **2012**, 1817. Available online: http://ma.ecsdl.org/content/MA2012-02/14/1817.short (accessed on 22 October 2019).
40. Vrubel, H.; Hu, X. Molybdenum Boride and Carbide Catalyze Hydrogen Evolution in both Acidic and Basic Solutions. *Angew. Chem. Int. Ed.* **2012**, 12703–12706. [CrossRef]
41. Wang, H.; Kong, D.; Johanes, P.; Cha, J.J.; Zheng, G.; Yan, K.; Liu, N. $MoSe_2$ and WSe_2 Nano fi lms with Vertically Aligned Molecular Layers on Curved and Rough Surfaces. *Nano Lett.* **2013**, *13*, 3426–3433. [CrossRef]
42. Kong, D.; Wang, H.; Cha, J.J.; Pasta, M.; Koski, K.J.; Yao, J.; Cui, Y. Synthesis of MoS_2 and $MoSe_2$ Films with Vertically Aligned Layers. *Nano Lett.* **2013**, *13*, 1341–1347. [CrossRef]
43. Merki, D.; Vrubel, H.; Rovelli, L.; Fierro, S.; Hu, X. Fe, Co, and Ni ions promote the catalytic activity of amorphous molybdenum sulfide films for hydrogen evolution. *Chem. Sci.* **2012**, *3*, 2515–2525. [CrossRef]
44. Environ, E. Hydrogen evolution catalyzed by MoS_3 and MoS_2 particle. *Energy Environ. Sci.* **2012**, *5*, 6136–6144.
45. Merki, D.; Fierro, S.; Vrubel, H.; Hu, X. Amorphous molybdenum sulfide films as catalysts for electrochemical hydrogen production in water. *Chem. Sci.* **2011**, *2*, 1262–1267. [CrossRef]
46. Wu, L.; Dzade, N.Y.; Yu, M.; Mezari, B.; van Hoof, A.J.F.; Friedrich, H.; de Leeuw, N.H.; Hensen, E.J.M.; Hofmann, J.P. Unraveling the Role of Lithium in Enhancing the Hydrogen Evolution Activity of MoS_2: Intercalation versus Adsorption. *ACS Energy Lett.* **2019**, *4*, 1733–1740. [CrossRef]
47. Zhang, J.; Liu, Y.; Sun, C.; Xi, P.; Peng, S.; Gao, D.; Xue, D. Accelerated Hydrogen Evolution Reaction in CoS_2 by Transition-Metal Doping. *ACS Energy Lett.* **2018**, *3*, 779–786. [CrossRef]
48. Wang, M.; Zhang, W.; Zhang, F.; Zhang, Z.; Tang, B.; Li, J.; Wang, X. Theoretical Expectation and Experimental Implementation of in Situ Al-Doped CoS_2 Nanowires on Dealloying-Derived Nanoporous Intermetallic Substrate as an Efficient Electrocatalyst for Boosting Hydrogen Production. *ACS Catal.* **2019**, *9*, 1489–1502. [CrossRef]
49. Li, Y.; Wang, H.; Peng, S. Tunable photodeposition of MoS_2 onto a composite of reduced graphene oxide and CdS for synergic photocatalytic hydrogen generation. *J. Phys. Chem. C* **2014**, *118*, 19842–19848. [CrossRef]
50. Xing, J.; Li, Y.H.; Jiang, H.B.; Wang, Y.; Yang, H.G. The size and valence state effect of Pt on photocatalytic H_2 evolution over platinized TiO_2 photocatalyst. *Int. J. Hydrog. Energy* **2014**, *39*, 1237–1242. [CrossRef]
51. Raut, P.; Li, S.; Chen, Y.M.; Zhu, Y.; Jana, S.C. Strong and Flexible Composite Solid Polymer Electrolyte Membranes for Li-Ion Batteries. *ACS Omega* **2019**, 4–10. [CrossRef] [PubMed]
52. Sun, J.; Wang, H.; Zhang, Y.; Zheng, Y.; Xu, Z.; Liu, R. Structure and luminescent properties of electrodeposited Eu^{3+}-doped CaF_2 thin films. *Thin Solid Film.* **2014**, *562*, 478–484. [CrossRef]
53. Liu, E.; Chen, J.; Ma, Y.; Feng, J.; Jia, J.; Fan, J.; Hu, X. Fabrication of 2D SnS_2 /g-C_3N_4 heterojunction with enhanced H_2 evolution during photocatalytic water splitting. *J. Colloid Interface Sci.* **2018**, *524*, 313–324. [CrossRef] [PubMed]
54. Yu, J.; Xu, C.Y.; Ma, F.X.; Hu, S.P.; Zhang, Y.W.; Zhen, L. Monodisperse SnS_2 nanosheets for high-performance photocatalytic hydrogen generation. *ACS Appl. Mater. Interfaces* **2014**, *6*, 22370–22377. [CrossRef] [PubMed]
55. Kong, C.; Min, S.; Lu, G. Dye-sensitized NiS_x catalyst decorated on graphene for highly efficient reduction of water to hydrogen under visible light irradiation. *ACS Catal.* **2014**, *4*, 2763–2769. [CrossRef]